KSCE Journal of Civil Engineering (2019) 23(2):879-888
Copyright ⓒ2019 Korean Society of Civil Engineers
DOI 10.1007/s12205-018-0100-0

Tunnel Engineering

pISSN 1226-7988, eISSN 1976-3808
www.springer.com/12205

A New Approach of Rock Cutting Efficiency Evaluation by using Plastic Energy Dissipation Ratio

Weiji Liu* and Xiaohua Zhu**

Received January 16, 2018/Revised July 31, 2018/Accepted September 30, 2018/Published Online December 17, 2018

Abstract

Polycrystalline Diamond Compact (PDC) bit is extensively used in oil & gas drilling, the rock cutting efficiency of PDC cutter directly determines the drilling efficiency and costs. Hence, it is crucial to evaluate the rock cutting efficiency of PDC cutters. The Mechanical Specific Energy (MSE) is used as an index for long periods of time to evaluate the rock cutting efficiency, however, the energy dissipation in rock breaking cannot be further calculated in details, leading to inaccuracy. To address this problem, the new concept of Plastic Energy Dissipation Ratio (PEDR) and its model are presented, a new approach for rock cutting efficiency evaluation by using PEDR is also put forward. Compared with MSE, the PEDR can determine the Optimum Depth of Cut (DOC) under various conditions. The theoretical analysis shows that the critical DOC, governing the transition of ductile to brittle failure mode, is the optimal cutting depth, having the smallest PEDR and highest rock cutting efficiency. The test and simulation of rock cutting are carried out to verify the PEDR model, and the PEDR under different DOC, cutting velocities and rake angles are depicted and discussed. The results can provide a theoretical basis for the design of PDC cutter and optimization of drilling parameters.

Keywords: *rock cutting efficiency, plastic energy dissipation ratio, mechanical specific energy, PDC bit, ductile-brittle failure*

1. Introduction

The low drilling efficiency and high drilling costs encountered in the oil and gas drilling, especially in the deep hard formations, are extremely challenging for engineers. The mechanical rock breaking is still frequently used in drilling, where the PDC bit is the main tool, and the rock cutting efficiency directly determines the drilling efficiency and drilling costs. To evaluate the rock cutting efficiency of PDC cutter has become a key for optimizing PDC cutter and drilling parameters, which is of vital importance for the improvement of drilling efficiency and reduction of drilling costs.

The Mechanical Specific Energy (MSE) is defined as the energy needed to break the unit volume of rock, it was first proposed by Teale (1965) for the evaluation of rock cutting efficiency and drilling efficiency. Subsequently, many researchers such as Zhou *et al.* (2012, 2014), Chen *et al.* (2015), Rajabov *et al.* (2012), Reyes *et al*. (2013), Mendoza (2013a), Munoz *et al.* (2016) did much valuable work about the rock cutting efficiency evaluation. Zhou *et al.* (2011, 2012, 2013a, 2013b, 2014) simulated the groove cutting using Finite Element Method (FEM), and analyzed the relationship between specific energy and cutting parameters, as well as the failure modes of rock and failure mode transition. Detournay and Tan (2002) have conducted about 20 cutting experiments under different confining pressure and initial pore pressure, they found that the specific energy depends only on bottom-hole pressure and not on the differential of bottom-hole pressure and pore pressure. Atici and Ersoy (2009), Altindag (2003) discussed the correlations between brittleness, destruction specific energy, and both cut ability and drill ability using the optimum data obtained from the laboratory experiments. Akbari *et al.* (2011, 2014a, 2014b) performed many experiments on Carthage marble limestone rock specimens in a high pressure cutting facility, and analyzed the effect of cutter geometry on the MSE and grain size distribution. Carrapatoso *et al.* (2013) investigated the cutting force responses and the relationship between MSE and cutting depth and rake angle by using the discrete element method. What is more, the research work about the interaction between cutter and rock also plays a significant role in well understanding the rock breaking mechanism and raising the Rate of Penetration (ROP), Karekal (2012) has analyzed the rock cutting process by using PFC2D, the results show that tensile dominate failure occurs when the depth of cut is shallow, and mixed tensile and shear failure occurs while the depth of cut is large. Zhang *et al.* (2015) studied the force response and crack propagation of rock in rock indentation by using PFC3D. Zhao *et al.* (2012) presented the numerical simulation of rock-cutter interaction, the effects of rake angle, blade angle and cutting depth on force response and crack development are discussed. In addition, the single cutter tests were carried out to analyze the mechanism of

*Lecturer, School of Mechatronic Engineering, Southwest Petroleum University, Chengdu 610500, China; Postdoctoral Research Station for Oil and Gas Engineering, Southwest Petroleum University, Chengdu 610500, China (E-mail: lwjzq1111@163.com)
**Professor, School of Mechatronic Engineering, Southwest Petroleum University, Chengdu 610500, China (Corresponding Author, E-mail: zxhth113@163.com)

rock cutting, and obtain the rock mechanical properties (Pei, 2012). Menezes *et al*. (2009, 2014a, 2014b) introduced an approach for simulating the fragmentation process in rock cutting by using the explicit element code LS-DYNA, the stress of rock and chip formation under various cutting depth and velocities are discussed. Chen *et al.* (2015) proposed a new cutter force model and explained why the precious cutting-area-based models failed to predict cutting forces. Bilgesu *et al.* (2008), Tulu (2009a, 2009b) and Sunal (2009) presented the rock cutting process by using the finite difference code FLAC-3D and analyzed the influence of temperature, pressure, formation and mud properties, bit design and drilling parameters on the force responses. Mendoza (2010, 2013a, 2013b) established a credible modeling framework for the well understanding of the rock cutting mechanics, the horizontal cutter force responses and fragmentation configuration is duplicated. According to the previous literature mentioned above, the MSE is used as an index for long periods of time to evaluate the rock cutting efficiency. However, the energy dissipation, including plastic energy dissipation and fracture energy dissipation, in rock breaking process cannot be calculated in details, besides, these research results show that the MSE decreases with the cutting depth increases, hence, the optimal cutting depth cannot be determined by using MSE as an index to evaluate the rock cutting efficiency because it is large enough to infinite when the magnitude of MSE is the smallest.

This study presents a new concept of PEDR and its theoretical model, and performs a new approach to evaluate rock cutting efficiency by using PEDR as an index. The experimental test and numerical simulation models of rock cutting are carried out to verify the theoretical model of PEDR. The results demonstrate that the critical DOC, which governs ductile to brittle failure of rocks, is the optimal cutting depth due to the smallest magnitude of PEDR and highest rock cutting efficiency.

2. Theoretical Analysis of PEDR

A transition of failure mode from ductile to brittle in rock cutting with the cutting depth increases. When the cutting depth is shallow, ductile failure of rock will take place, which accompanies by the generation of plastic zone beneath and beside the cutter, as Fig. 1 depicts. In contrast, brittle failure occurs as the cutting

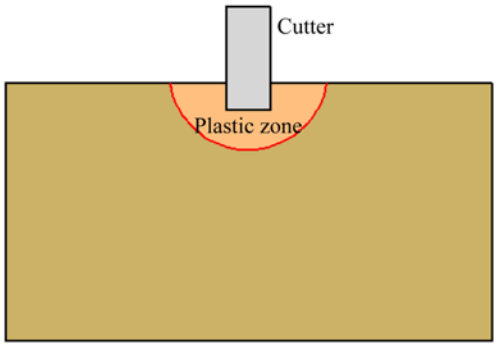

Fig. 1. The Schematic Diagram of Ductile Failure in Rock Cutting

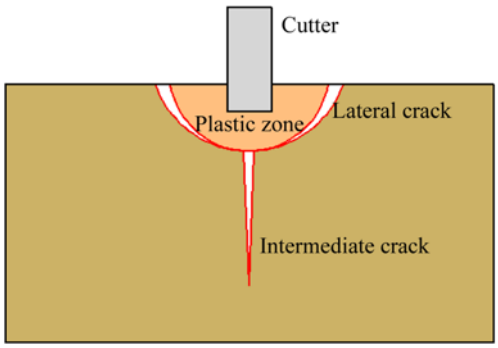

Fig. 2. The Schematic Diagram of Brittle Failure in Rock Cutting

depth increased exceeds a certain value with the formation of both plastic zone and fractured zone which includes intermediate crack and lateral crack, Fig. 2 shows a schematic plot of the formed cracks.

Assuming the rock fails in ductile mode during cutting with a shallow DOC, when considering the influence of rake angle, the cutting force can be expressed as:

$$F_c = \eta \sigma_c A \tag{1}$$

where σ_c presents the Uniaxial Compressive Strength (UCS) of rock sample, η denotes the constant which associated with the rake angle γ_b of cutter, and A presents the contact area between cutter and rock.

The energy consumed in ductile failure of rock equals to the product of cutting force and displacement:

$$E_{dp} = F_c \Delta l = \eta \sigma_c A \Delta l \tag{2}$$

In addition, the energy consumed in the sliding friction between the cutter and rock surface can be written as:

$$E_{dz} = \mu \sigma_f A_f \Delta l \tag{3}$$

where μ presents the friction coefficient between the cutter and rock surface; $\sigma_f = k_0 H \sqrt{H/E}$; k_0 presents a constant coefficient related to the contact stress σ_f and rock hardness H; E is the elastic modulus of rock material; $A_f = w_c l_2$ is the contact area between wear flat and rock surface; and l_2 is the length of wear flat (Arcona and Dow, 1998).

As a result, the total energy which consumed in ductile dominated failure of rock material equals to the sum of Eq. (2) and Eq. (3):

$$E_d = E_{dp} + E_{dz} \tag{4}$$

The removed volume of rock material in ductile rock cutting for a certain cutting displacement of Δl is given as:

$$V_d = A \Delta l \tag{5}$$

For the cutter without wear, which has the sharp edge, the magnitude of E_{dz} cannot be considered during cutting, thus, the total energy of E_d equals to E_{dp} and MSE calculated by dividing E_d by V_d:

$$\mu_{bp} = E_d / V_d = E_{dp} / V_d = \eta \sigma_c A \Delta l / A \Delta l = \eta \sigma_c \tag{6}$$

Figure 2 presents that when the rock fails in brittle mode, the lateral cracks and intermediate cracks will generate, causing a lateral and vertical damage zone. The cutting force is related to the DOC by a power law $F_c \propto \sqrt{d}$. As shown in the figure, the lateral cracking zone is a half cylinder with radius c_1, thus, the total volume of removed rock for brittle failure mode is (Bifano *et al.,* 1991):

$$V_b = \frac{\pi}{2} c_1^2 \Delta l \tag{7}$$

where c_1 and c_m present the length of lateral crack and median crack, respectively (Bifano *et al*., 1991).

$$c_1 \cong c_m / k_1 \tag{8}$$

where k_1 presents a scaling constant, there exist a power law between c_m and the normal force F_t; $c_m \propto F_t^{2/3}$; and the normal force can be scaled to the DOC by $F_t \propto d^2$. According to the above results, it can be obtained that (Bifano *et al*., 1991; Marshall, 1983):

$$c_1 \propto d^{4/3} \tag{9}$$

The energy consumed on the brittle fractures is mainly dependent on the specific surface energy which is required for the generation of unit surface area, and the fractured surface area can be written as (Bifano *et al*., 1991):

$$A_s = (2\pi c_1 + 2c_m)\Delta l \tag{10}$$

Hence, the fracture energy is given as:

$$E_{df} = A_s G_f = (2\pi c_1 + 2c_m) G_f \Delta l \tag{11}$$

where G_f denotes the specific surface energy.

Besides, the plastic energy consumed is given as:

$$E_{dp} = \lambda \sigma_y V_p = \frac{\pi}{4} \lambda \sigma_y c_1^2 \Delta l \tag{12}$$

where V_p denotes the volume of plastically deformed zone, it equals $V_p = \pi/4 c_1^2 \Delta l$, and the total energy equals to the sum of fracture energy and plastic energy for brittle failure of rock:

$$E_d = E_{df} + E_{dp} = \left[(2\pi c_1 + 2c_m) G_f + \frac{\pi}{4} \lambda \sigma_y c_1^2 \right] \Delta l \tag{13}$$

The MSE can be caculated by dividing the total energy E_d consumed in brittle cutting by the volume V_b removed by the brittle fractures, it can be expressed as:

$$\begin{aligned} \mu_{bf} &= E_d / V_b = \left[(2\pi c_1 + 2c_m) G_f + \frac{\pi}{4} \lambda \sigma_y c_1^2 \right] \Delta l \Big/ \frac{\pi}{2} c_1^2 \Delta l \\ &= K_b d^{-4/3} + K_P \end{aligned} \tag{14}$$

Equations (6) and (14) combine defined a piecewise function to describe ductile to brittle failure transition of rock by using MSE with respect to DOC:

$$\mu_b = \begin{cases} \eta \sigma_c & d < d_c \\ K_b d^{-4/3} + K_P & d > d_c \end{cases} \tag{15}$$

where K_b denotes the influence factor which have a bearing on the cutting geometry and material properties, such as G_f, K_{IC}, H, E, c_1 and c_m, and K_p is the energy needed to generate the plastic deformation zone.

The magnitude of MSE is independent of DOC in the ductile cutting process, keeping a constant. When the cutting depth exceeds a certain value, the magnitude of MSE will decrease as the DOC increases, and MSE equals to K_p when the DOC is infinite. The total work done by the cutter is consumed on the plastic zone of rock and the friction between cutter and rock surface in ductile dominated failure (the energy consumed on the friction is ignored due to the cutter is assumed with the sharp cutting edge in this study). However, in the brittle dominated failure, the total work is consumed on the plastic zone, friction and fracture surface.

The theoretical model of MSE for brittle dominated failure is just shown as Eq. (14), it consists of two items, $K_b d^{-4/3}$ presents the energy consumed in the fracture surface, and K_P is the energy consumed in plastic zone. The brittle failure mode of rock is expected during rock cutting process due to the large MSE and low rock cutting efficiency of ductile failure mode. The plastic energy dissipation induces the plastic deformation or powdery and smaller chips generation, while the fracture energy dissipation causes the formation of relatively big chip, small magnitude of MSE and high rock cutting efficiency. Therefore, the magnitude of PEDR plays an essential role in the rock cutting efficiency improvement in the brittle dominated failure of rock, the larger the PEDR the lower the rock cutting efficiency. The index of PEDR is proposed to evaluate the rock cutting efficiency in present study, defined as the ratio of $K_P/K_b d^{-4/3}$. This new approach can provide a theoretical basis for the design of PDC cutter and optimization of cutting parameters.

The PEDR is calculated with Eq. (16), the PEDR is only suitable for brittle failure mode of rock because the magnitude of PEDR remains 1 in ductile failure. This study investigates the optimal cutting parameters which has the smallest PEDR and highest rock cutting efficiency. Figure 3 plots the PEDR with regard to different cutting depth, the PEDR equals to 1 both when the cutting depth is shallow and infinite, which the

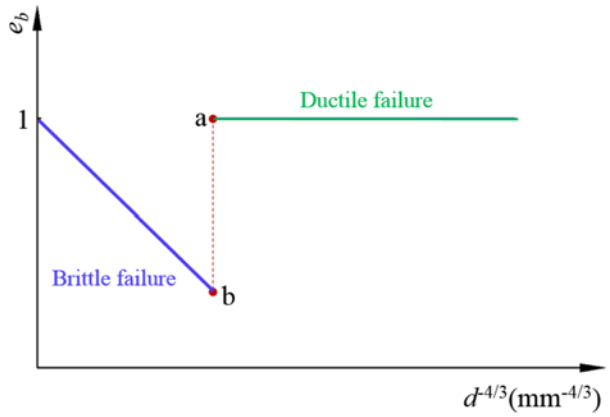

Fig. 3. The PEDR Versus $d^{-4/3}$

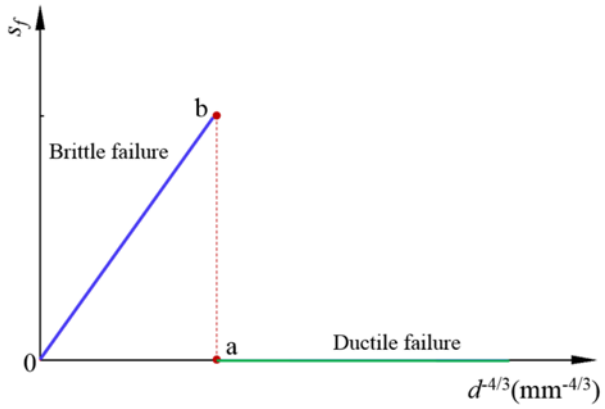

Fig. 4. The FEDR Versus $d^{-4/3}$

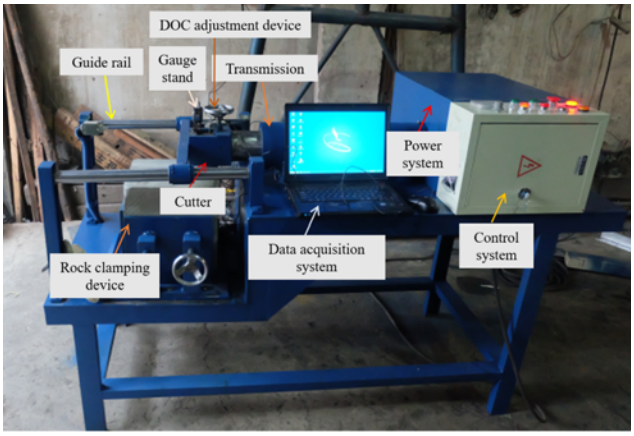

Fig. 5. The Experiment Facility of Rock Cutting

rock cutting efficiency is the smallest at this situation. The magnitude of PEDR will be abruptly changed as the cutting depth increases, just as the red point a to b. With the cutting depth increase, the PEDR will also increase until it equals to 1. The magnitude of PEDR at point b is smallest and the rock cutting efficiency is the highest, the corresponding cutting depth of point b is just the critical DOC. Figure 4 presents the relationship between Fracture Energy Dissipation Ratio (FEDR) and cutting depth, it indicates that the magnitude of FEDR at point b is the highest.

According to the above analysis, the cutting depth at point b (it can be called as critical DOC) is the optimal cutting depth which has the smallest magnitude of PEDR and highest rock cutting efficiency. This is the progress of PEDR in comparison with MSE. The theoretical model of PEDR can be expressed as:

$$e_b = \begin{cases} 1 & d < d_c \\ K_P / (K_b d^{-4/3} + K_P) & d > d_c \end{cases} \tag{16}$$

Similarly, the FEDR can be written as:

$$e_f = \begin{cases} 0 & d < d_c \\ K_b d^{-4/3} / (K_b d^{-4/3} + K_P) & d > d_c \end{cases} \tag{17}$$

3. Experimental Study of PEDR

The experiment of rock cutting is designed for PEDR under different conditions (various cutting depths, cutting velocities and rake angles) as Fig. 5 shows. The cutting velocity is slow and adjustable, the minimum scale of DOC is 0.01 mm. The six surfaces of the rock specimen are polished in order to improve the precision of results, the cutting force history is monitored by the data acquisition system during the cutting process. The results obtained from the experiment tests will be used to verify and supply the theoretical analysis of PEDR.

3.1 Results of Experiment Tests

Two types of rock are used as the specimens in rock cutting, red sandstone and black sandstone. The physical parameters of red sandstone and black sandstone are obtained through the rock mechanical tests. For the red sandstone the Elastic modulus is 3748.1 MPa, the Poisson's ratio is 0.314, the UCS is 25 MPa and BTS is 1.31 MPa, and for the black sandstone the Elastic modulus is 9100.5 MPa, the Poisson's ratio is 0.143, the UCS is 82 MPa and BTS is 2.97 MPa (Liu *et al*., 2018).

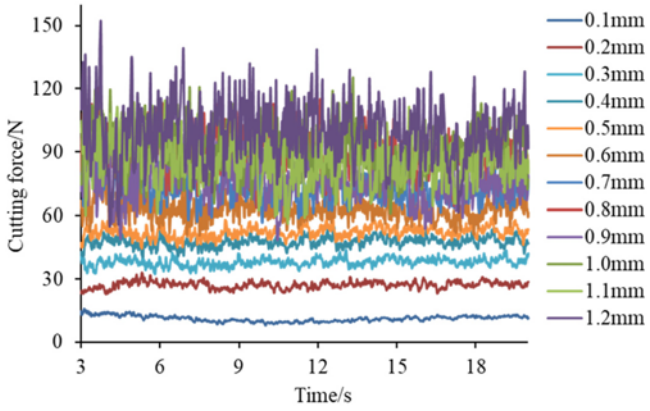

Fig. 6. The Cutting Force Responses under Different Cutting Depth for Red Sandstone

Figure 6 plots the cutting force responses under different cutting depths, the cutting depth range from 0.1 mm to 1.2 mm with an interval of 0.1 mm, the cutting velocity is 16 mm/s and the rake angle is 15º. The results illustrate that the cutting force increases with the DOC. The curve of cutting force is smooth with small fluctuation when the DOC keeps in a shallow level. However, the fluctuation of cutting force maintains a high level when the DOC exceeds a certain value.

Figure 7 shows the morphology of rock specimen during and after the cutting process. As Fig. 7(a) shows, the formed chips heaped in front of the cutter surface and distributed at the both sides of the cutter eventually. The Fig. 7(b) depicts the grooves caused by rock cutting.

Figure 8 shows the relationship between MSE and DOC for red sandstone, the magnitude of MSE with respect to d is plotted in Fig. 8(a), and the relationship between MSE and $d^{-4/3}$ is presented in Fig. 8(b). Just as Fig. 8(a) shows, the MSE is almost proportion to d, the MSE decreases with the increase of d, the

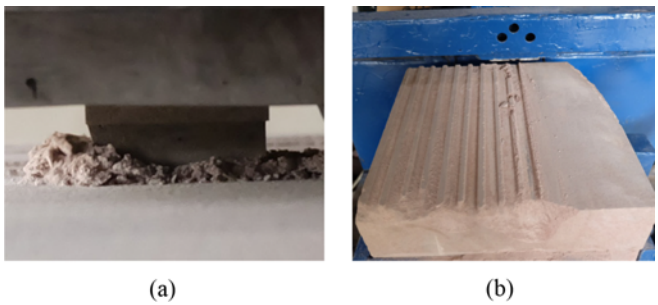

(a) (b)

Fig. 7. The Morphology of Rock Specimen During and after the Cutting for Red Sandstone: (a) the Distribution of Chips, (b) the Formed Grooves

lager the cutting depth the higher the rock cutting efficiency. Thus, the optimal cutting depth cannot be determined by using the MSE as an index to identify the rock cutting efficiency. The Fig. 8(b) shows a transition point which divides the MSE fitting curve into two parts: One is the brittle failure area, the MSE can be expressed by a straight line with respect to $d^{-4/3}$ with a certain value of slope and intercept; the another is ductile failure area, the magnitude of MSE almost maintains a constant. Fig. 8(a) and Fig. 8(b) are presented a totally different relationship between MSE and cutting depth, which will result in different cognitions on rock cutting mechanism.

The results of MSE plotted in Fig. 8(b) are in good agreement with the theoretical analysis, which can be fitted as the straight blue line with a slope of 1.71 and an intercept of 5.4, just as y = 1.71x + 5.4. Comparing with the Eq. (6), it indicates that K_b = 1.71x and K_p = 5.4, correspondingly. Therefore, the magnitude of PEDR and FEDR can be calculated, just shown in Fig. 9. The Fig. 9(a) depicts the results of PEDR, the magnitude of PEDR equals to 1 in ductile failure just as the green line shows, and it increases with the cutting depth decreases in brittle dominated failure, just as the blue line shows. These two fitted lines are not continuous but piecewise, the PEDR is the smallest and rock cutting efficiency is the highest when the cutting depth equals the critical DOC. The results of FEDR are plotted in Fig. 9(b), the magnitude of FEDR is the largest at the critical DOC.

The critical DOC is the optimal cutting depth in rock cutting process, which can be obtained if the drilling parameters are well controlled in the oil gas drilling, and the drilling efficiency will be improved sharply and drilling cost will be reduced.

The PEDR under different cutting velocities are plotted in Fig. 10 and Fig. 11, the cutting velocity is 8 mm/s and 24 mm/s respectively. In comparison with Fig. 9(a), it indicates that the cutting velocity has limited influence on the PEDR and critical DOC. The PEDR under different rake angles are presented in

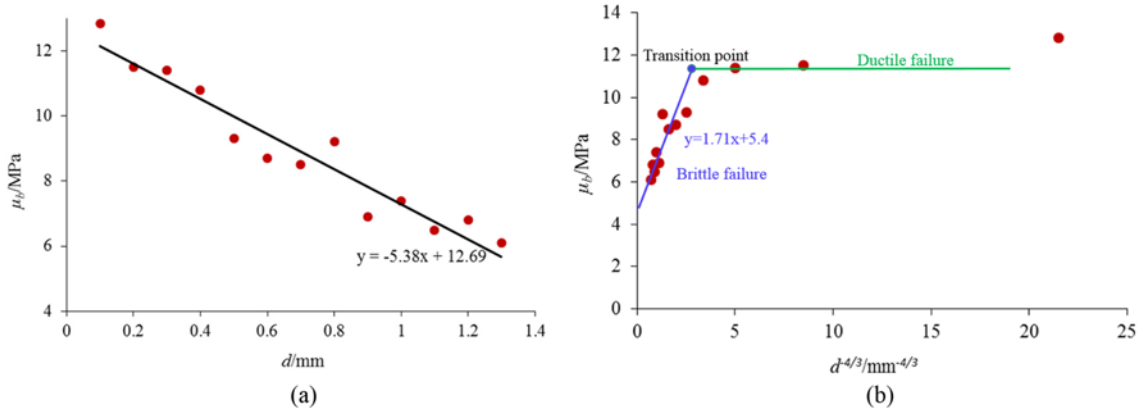

Fig. 8. The Relationship between MSE and Cutting Depth for Red Sandstone: (a) MSE Versus *d*, (b) MSE Versus $d^{-4/3}$

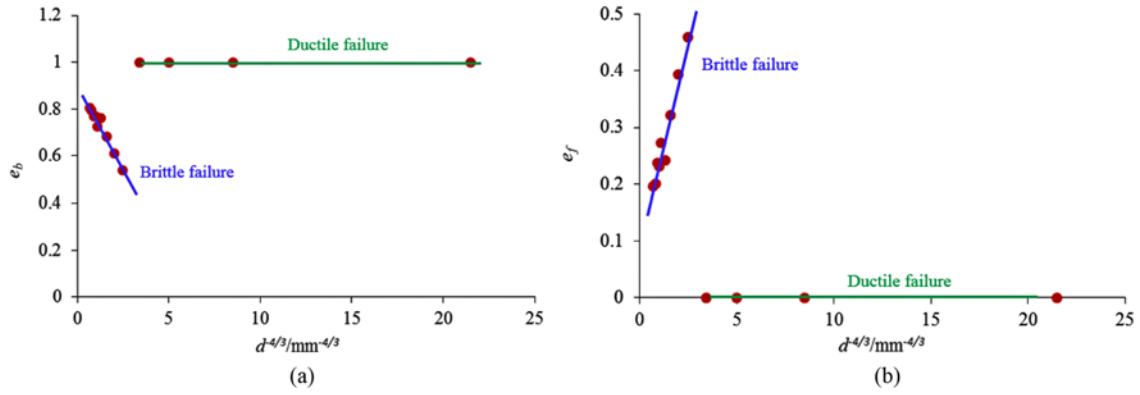

Fig. 9. The Relationship between PEDR (FEDR) and Cutting Depth for Red Sandstone: (a) PEDR Versus *d*, (b) FEDR Versus *d*

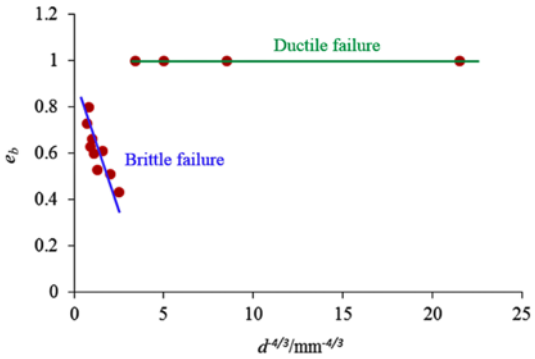

Fig. 10. The Relationship between PEDR (FEDR) and Cutting Depth for Red Sandstone: (a) PEDR versus *d*, (b) FEDR versus *d*

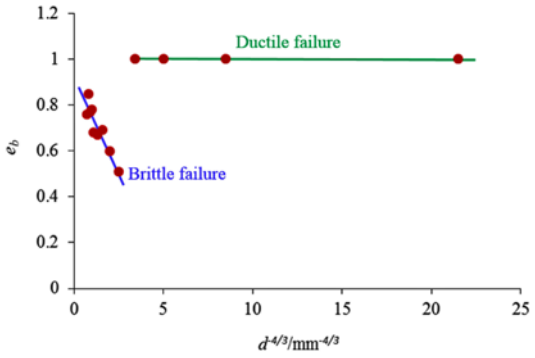

Fig. 11. PEDR versus *d* with Cutting Velocity 24 mm/s

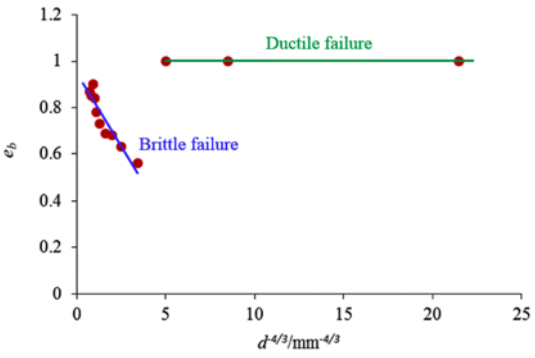

Fig. 12. PEDR versus *d* with Rake Angle 0º

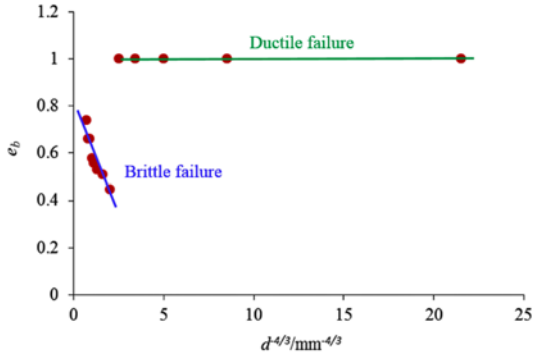

Fig. 13. PEDR versus *d* with Rake Angle 25º

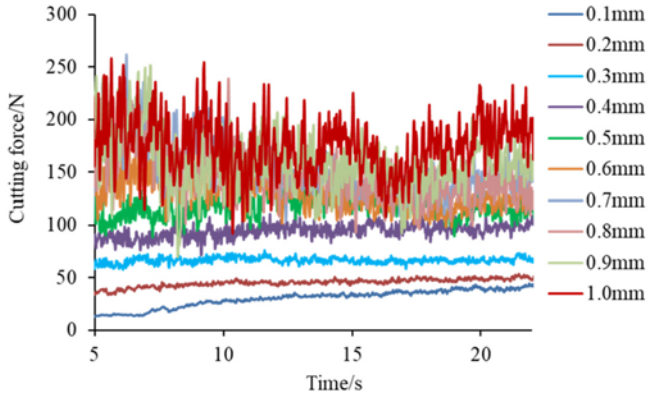

Fig. 14 The Cutting Force Responses under different Cutting Depth for Black Sandstone

Fig. 15. The Morphology of Rock Specimen During and after the Cutting for Black Sandstone: (a) the Distribution of Chips, (b) the Formed Grooves

Fig. 12 and Fig. 13, the rake angle is 0º and 25º respectively. The smaller the rake angle is the smaller the critical DOC would be, which means the less Weight On Bit (WOB) is needed for the smaller rake angle of cutter to obtain the higher PEDR and drilling efficiency.

Similarly, Fig. 14 illustrates the cutting force responses for black sandstone under different cutting depth. Figure 15 shows the morphology of rock specimen during and after the cutting process.

Figure 16 shows the relationship between MSE and cutting depth, the MSE with respect to *d* is plotted in Fig. 16(a), the magnitude of MSE almost decreases with the *d* increases, it is similar to the results of red sandstone. The relationship between MSE and $d^{-4/3}$ is presented in Fig. 16(b), the results of MSE in brittle failure of rock can be fitted as y = 5.8x + 8.7, as a result, there exists K_b = 5.8x and K_p = 8.7 while comparing with the Eq. (15). The relationship between PEDR (FEDR) and cutting depth are shown in Fig. 17, the critical DOC for black sandstone is larger in comparison with the results of red sandstone, it is closely related to the brittleness of rocks.

4. Numerical Simulation Study of PEDR

In order to verify the theoretical model of PEDR further, the discrete element method (PFC2D) is carried out to simulate the rock cutting process in this section, the rock cutting model is just

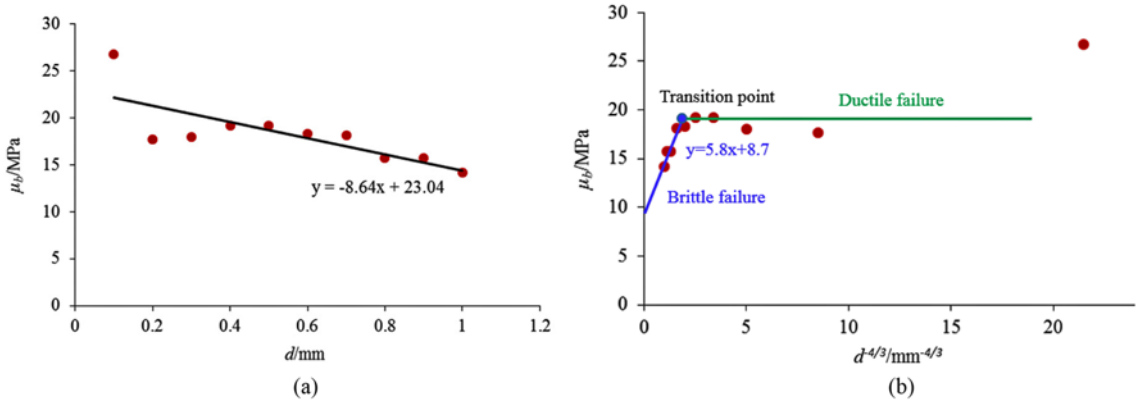

Fig. 16. The Relationship between MSE and Cutting Depth for Black Sandstone: (a) MSE versus d, (b) MSE versus $d^{-4/3}$

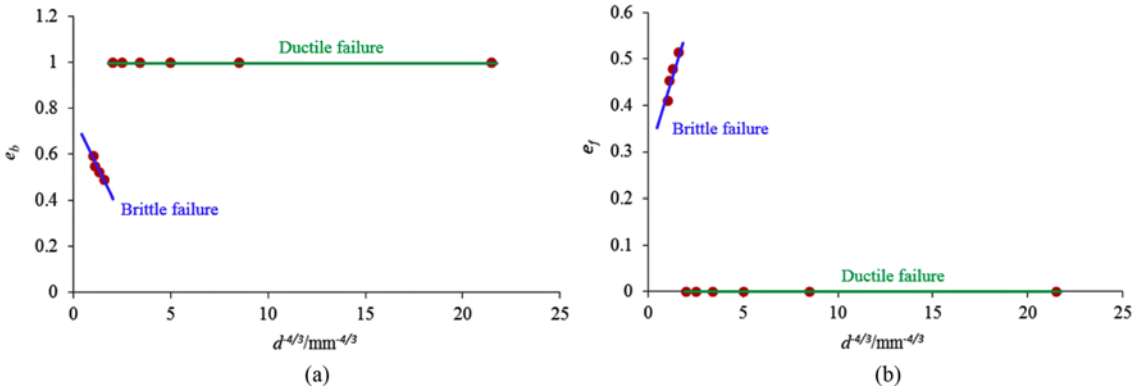

Fig. 17. The Relationship between PEDR (FEDR) and Cutting Depth for Black Sandstone: (a) PEDR versus $d^{-4/3}$, (b) FEDR versus $d^{-4/3}$

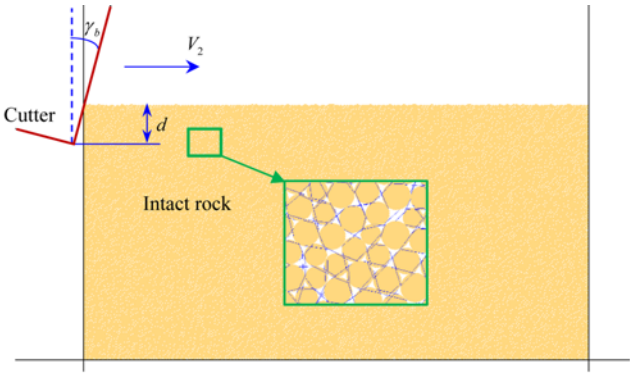

Fig. 18. The Rock Cutting Model of Numerical Simulation

Table 1. Micro-properties for the Rock Model

Particle		Parallel bond	
μ_1	0.5	$\bar{\lambda}$	1.0
R_{min} (mm)	0.075	pbsn (MPa)	20 ± 2
R_{max}/R_{min}	1.66	pbss (MPa)	20 ± 2
E_c (GPa)	4	pbm (GPa)	4
k_n/k_s	5.5	pbk	5.5

shown in Fig. 18, it consists of a cutter and a rock model with the length and width of 40 mm and 20 mm respectively. The rock model has 26 635 particles, and the radius of those particles are range from 0.075 mm to 0.1125 mm, the average radius of the particles is denoted by R. The parallel bonds in PFC2D are utilized to bond the separate particles, just as the blue lines shown in the enlarged view of rock model. The results from the UCS and Brazilian Tensile Strength (BTS) tests of red sandstone are used to calibrate the micro-properties of the particles and bonds in the rock model, Table 1 list the calibrated micro-properties, the calibration process is described in detail in the reference (Liu *et al*., 2018), thus, it is not duplicated in present study. Parallel bond model is a more realistic for rock-like materials because it can transmit both a force and a moment (Itasca, 2002; Zhu *et al*., 2017). The rectangular rock model is restricted by three frictionless walls, the bottom of rock model remains fixed in vertical direction, the left and right sides remain fixed in horizontal direction. The cutting velocity, V, remains constant with the cutting depth d and the rake angle of γ_b.

Figure 19 presents the formation of fracture and rock chip in rock cutting process, the micro-cracks generate when the external load applied on the particles exceeds the bond strength during the interaction of cutter and rock, the red lines represent the particle bonds fail in tensile force, and the blue lines represent the particle bonds fail in shear force.

In this section, a large number of rock cutting simulations are conducted to obtain the MSE and PEDR (FEDR). Figure 20

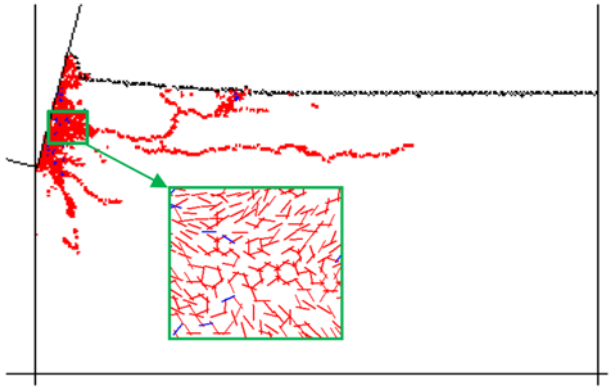

Fig. 19. The Breakage of Parallel Bonds in Rock Cutting

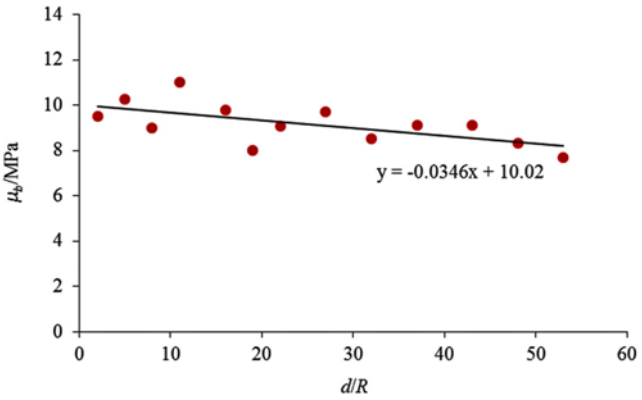

Fig. 20. The Relationship between MSE and Cutting Depth

shows the relationship between MSE and cutting depth d, the MSE decreases with the DOC increases, similar to the results of experiment tests. Figure 21 shows the PEDR (FEDR) with respect to cutting depth, the cutting velocity is 0.3 m/s and the rake angle is 15º. The numerical simulation results show that the PEDR will be abruptly changed as the cutting depth increases. With the increase of cutting depth, the PEDR increases until it almost equals 1 (it is different to the theoretical calculation results because the cutting depth is impossible to reach infinite large in actual condition). The magnitude of PEDR at the critical DOC is smallest and the rock cutting efficiency is the highest, the results obtained from the numerical simulation are in good agreement with the theoretical analysis and experiment tests. In addition, the rock cutting simulations under various cutting velocities and rake angles are also performed, but it is not been illustrated here due to the results observed in the simulations are similar to the experiment tests.

5. Conclusions

The new concept of PEDR is proposed in present study and the approach of rock cutting efficiency evaluation by using it as an index is also discussed. Compared with MSE the PEDR can be used to determine the optimum DOC under various conditions.

Theoretical analysis performed on PEDR shows that the critical DOC, which governs ductile to brittle failure of rocks, is the optimal cutting depth due to the smallest magnitude of PEDR and highest rock cutting efficiency. The critical DOC can be obtained if the drilling parameters are well controlled in the oil gas drilling, and the drilling efficiency will be improved and drilling cost will be also reduced.

The experimental test and numerical rock cutting models are conducted, and the PEDR model is verified by the results observed from the experiments and simulations, the PEDR under different DOC, cutting velocities and rake angles are discussed. The cutting velocity has limited influence on the PEDR and critical DOC. The smaller the rake angle is the smaller the critical DOC would be, which means the less WOB is needed for the smaller rake angle of cutter to obtain the higher PEDR and drilling efficiency.

The new approach of rock cutting efficiency evaluation using PEDR as an index can provide progress in the design of PDC bit and optimization of drilling parameters.

Acknowledgements

This study is supported by the National Natural Science Foundation of China (Grant No.51674214), International Cooperation Project of Sichuan Science and Technology Plan

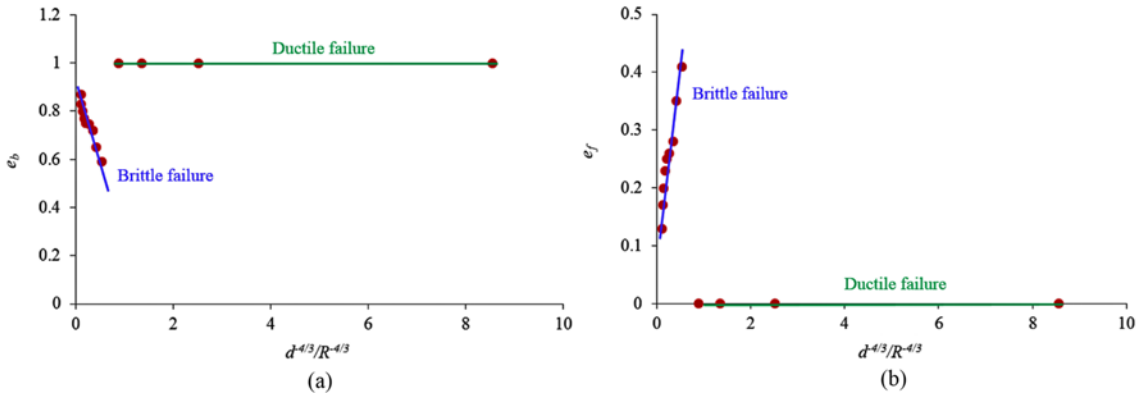

Fig. 21. The Results of PEDR (FEDR) with respect to Cutting Depth: (a) PEDR versus $d^{-4/3}$, (b) FEDR versus $d^{-4/3}$

(2016HH0008), Youth Science and Technology Innovation Research Team of Sichuan Province (2017TD0014). Such supports are greatly appreciated by the authors.

References

Akbari, B. (2011). *Polycrystalline diamond compact bit-rock interaction*, Memorial University of Newfoundland.

Akbari, B., Miska, S., Yu, M., and Ozbayoglu, E. (2014a). *Relation between the mechanical specific energy, cuttings morphology, and PDC cutter geometry*, ASME Paper No. OMAE2014-24708, pp. V005T11A038, DOI: 10.1115/OMAE2014-24708.

Akbari, B., Miska, S. Z., Yu, M., and Rahmani, R. (2014b). "The effects of size, chamfer geometry, and back rake angle on frictional response of PDC cutters." *48th US Rock Mechanics/Geomechanics Symposium,* American Rock Mechanics Association, ARMA 14-7458, Minneapolis, MN, SUA.

Altindag, R. (2003). "Correlation of specific energy with rock brittleness concepts on rock cutting." *Journal of the South African Institute of Mining and Metallurgy*, Vol. 103, No. 3, pp.163-171.

Arcona, C. and Dow, T. A. (1998). "An empirical tool force model for precision machining." *Journal of Manufacturing Science and Engineering*, Vol. 120, No. 4, pp. 700-707, DOI: 10.1115/1.2830209.

Atici, U. and Ersoy, A. (2009). "Correlation of specific energy of cutting saws and drilling bits with rock brittleness and destruction energy." *Journal of Materials Processing Technology*, Vol. 209, No. 5, pp. 2602-2612, DOI: 10.1016/j.jmatprotec.2008.06.004.

Bifano, T. G., Dow, T. A., and Scattergood, R. O. (1991). "Ductile-regime grinding: a new technology for machining brittle materials." *Journal of Manufacturing Science and Engineering*, Vol. 113, No. 2, pp. 184-189, DOI: 10.1115/1.2899676.

Bilgesu, I., Sunal, O., Tulu, I. B., Heasley, K. A. (2008). "Modeling rock and drill cutter behavior." *42nd US Rock Mechanics Symposium & 2nd US-Canada Rock Mechanics Symposium*, San Francisco, CA, USA.

Carrapatoso, C., Fontoura, S. A. B., Martinez, I. M. R., Inoue, N., Lourenço, A., and Curry, D. (2013). "Simulation of single cutter experiments in evaporite through discrete element method." In *ISRM Internation Symposium - EUROCK 2013*, International Society for Rook Mechanics and Rook Engineering, Wroclaw, Poland .

Chen, S., Grosz, G., Anderle, S., Arfele, R., and Xun, K. (2015). "The role of rock-chip removals and cutting-area shapes in polycrystalline-diamond-compact-bit design optimization." *SPE Drilling & Completion, SPE 171833,* DOI: 10.2118/17183 3-PA.

Detournay, E. and Tan, C. P. (2002). "Dependence of drilling specific energy on bottom-hole pressure in shales." *SPE/ISRM Rock Mechanics Conference,* Society of Petroleum Engineers, SPE/ISRM 78221, DOI: 10.2118/78221-MS.

Itasca, C.G. (2002). *Users' manual for particle flow code in 2 dimensions (PFC2D),* Minneapolis, Minnesota, USA.

Karekal, S. (2012). "Modeling Rock chipping process in linear drag cutting mode." *ISRM International Symposium - EUROCK 2012*, International Society for Rock Mechanics, Stockholm, Sweden.

Liu, W., Zhu, X., and Jing, J. (2018). "The analysis of ductile-brittle failure mode transition in rock cutting." *Journal of Petroleum Science and Engineering*, Vol. 163, pp. 311-319, DOI: 10.1016/j.petrol.2017.12.067.

Marshail, D. B. (1983). "Geometrical effects in elastic/plastic indentation." *Journal of the American Ceramic Society*, Vol. 67, No. 1, pp. 57-60, DOI: 10. 1111/j.1151-2916.1984.tb19148.x.

Mendoza, R. J. A. (2010). *Modeling rock cutting using DEM with crushable particles*, PhD Thesis, University of Pittsburgh, Pittsburgh, PA, USA.

Mendoza, R. J. A. (2013). *Considerations for discrete element modeling of rock cutting*, PhD Thesis, University of Pittsburgh, Pittsburgh, PA, USA.

Mendoza, J. A., Gamwo, I. K., Zhang, W., and Lin, J. S. (2013b). "Considerations for discrete modeling of rock cutting." *45th US Rock Mechanics/Geomechanics Symposium*, American Rock Mechanics Association, ARMA-11-210, San Francisco, CA, USA.

Menezes, P. L., Lovell, M. R., Avdeev, I. V., and Higgs, C. F. (2014a). "Studies on the formation of discontinuous rock fragments during cutting operation." *International Journal of Rock Mechanics and Mining Sciences*, Vol. 71, pp. 131-142, DOI: 10.1016/j. ijrmms. 2014.03.019.

Menezes, P. L., Lovell, M. R., Avdeev, I. V., and Higgs, C. F. (2014b). "Studies on the formation of discontinuous chips during rock cutting using an explicit finite element model." *The International Journal of Advanced Manufacturing Technology*, Vol. 70, Nos. 1-4, pp. 635-648, DOI: 10.1007/s00170-013-5309-y.

Menezes, P. L., Lovell, M. R., Lin, J. S., and III, C. F. H. (2009). "Finite Element modeling of discontinuous chip formation during rock cutting." *ASME/STLE 2009 International Joint Tribology Conference,* American Society of Mechanical Engineers, pp. 463-465, DOI: 10.1115/IJTC2009-15197.

Munoz, H., Taheri, A., and Chanda, E. K. (2016). "Rock drilling performance evaluation by an energy dissipation based rock brittleness index." *Rock Mechanics and Rock Engineering*, Vol. 49, No. 8, pp. 3343-3355, DOI: 10.1007/s00603-016- 0986-0.

Pei, J. Y. (2012). "Interpretation of single cutter tests for rock mechanical properties." *46th US Rock Mechanics/Geomechanics Symposium*, American Rock Mechanics Association, ARMA 12-142, Chicago, IL, USA.

Rajabov, V., Miska, S. Z., Mortimer, L., Yu, M., and Ozbayoglu, M. E. (2012). "The effects of back rake and side rake angles on mechanical specific energy of single PDC cutters with selected rocks at varying depth of cuts and confining pressures." *IADC/SPE Drilling Conference and Exhibition*, Society of Petroleum Engineers, DOI: 10.2118/151406-MS

Reyes, M. I., Fontoura, S., Inoue, N., Carrapatoso, C., Lourenco, A., and Curry, D. (2013). "Simulation of single cutter experiments in evaporites through finite element method." *SPE/IADC Drilling Conference*, Society of Petroleum Engineers, SPE/IADC 163504.

Sunal, O. (2009). *Parametric study of a single PDC cutter with a numerical model*, MSc Thesis, West Virginia University, Morgantown, WV, USA.

Teale, R. (1965). "The concept of specific energy in rock drilling." *International Journal of Rock Mechanics and Mining Sciences & Geomechanics Abstracts*, Vol. 2, No. 1, pp. 57-73, DOI: 10.1016/0148-9062(65)90016-1.

Tulu, I. B. (2009a). *Modeling PDC cutter rock interaction*, MSc Thesis, West Virginia University, Morgantown, WV, USA.

Tulu, I. B. and Heasley, K. A. (2009b). "Calibration of 3D cutter-rock model with single cutter tests." *43rd US Rock Mechanics Symposium & 4th US-Canada Rock Mechanics Symposium*, American Rock Mechanics Association, ARMA 09-160, Asheville, NC, USA.

Zhang, Q. Q., Han, Z. N., Zhang, M. Q., and Zhang, J. G. (2015). "Prediction of tool forces in rock cutting using discrete element method." *Electronic Journal of Geotechnical Engineering*, Vol. 20, No. 5, pp. 1607-1625.

Zhao, D., Liu, J. Q., and Guo, W. (2012). "The simulation of cutter-rock

interaction in PFC." *Applied Mechanics and Materials*, Vols. 170-173, pp. 3385-3389, DOI: 10.4028/www.scientific.net/AMM.170-173.3385.

Zhou, Y. (2013b). *Numerical modeling of rock drilling with finite elements,* PhD Thesis, University of Pittsburgh, Pittsburgh, PA, USA.

Zhou, Y. and Lin, J. S. (2013a). "On the critical failure mode transition depth for rock cutting." *International Journal of Rock Mechanics and Mining Sciences*, Vol. 62, pp. 131-137, DOI: 10.1016/j.ijrmms.2013.05.004.

Zhou, Y. and Lin, J. S. (2014). "Modeling the ductile–brittle failure mode transition in rock cutting." *Engineering Fracture Mechanics*, Vol. 127, pp. 135-147, DOI: 10.1016/j.engfracmech.2014.05.020.

Zhou, Y., Jaime, M. C., Gamwo, I. K., Zhang, W., and Lin, J. S. (2011). "Modeling groove cutting in rocks using finite elements." *45th US Rock Mechanics/Geomechanics Symposium*, American Rock Mechanics Association, ARMA 11-209, San Francisco, CA, USA.

Zhou, Y., Zhang, W., Gamwo, I. K., Lin, J. S., Eastman, H., Whipple, G., and Gill, M. (2012). "Mechanical specific energy versus depth of cut." *46th US Rock Mechanics/Geomechanics Symposium*, American Rock Mechanics Association, ARMA 12-622, Chicago, IL, USA.

Zhu, X., Liu, W., and He, X. (2017). "The investigation of rock indentation simulation based on discrete element method." *KSCE Journal of Civil Engineering*, Vol. 21, No. 4, pp. 1201-1212, DOI: 10.1007/s12205-016-0033-4.